Supplementary Information

Cellular Active *N*-Hydroxyurea FEN1 Inhibitors Block Substrate Entry to the Active Site

Jack C. Exell,[1,6] Mark J. Thompson,[1] L. David Finger,[1] Steven J. Shaw,[1] Judit Debreczeni,[2] Thomas A. Ward,[4] Claire McWhirter,[2] Catrine L. B. Siöberg,[5] Daniel Martinez Molina,[5] W. Mark Abbott,[2] Clifford D. Jones,[3] J. Willem M. Nissink,[3,*] Stephen T. Durant[4,*] and Jane A. Grasby.[1,*]

[1]*Centre for Chemical Biology, Department of Chemistry, Krebs Institute, University of Sheffield, Sheffield, S3 7HF, UK*

[2]*Discovery Sciences, Innovative Medicines and Early Development Biotech Unit, AstraZeneca, Unit 310 (Darwin Building), Cambridge Science Park, Milton Road, Cambridge, CB4 0WG, UK.*

[3]*Chemistry, Oncology, Innovative Medicines and Early Development Biotech Unit, AstraZeneca, Unit 310 (Darwin Building), Cambridge Science Park, Milton Road, Cambridge, CB4 0WG, UK and Alderley Park, Cheshire, SK10 4TG, UK.*

[4]*Bioscience, Oncology, Innovative Medicines and Early Development Biotech Unit, CRUK Cambridge Institute, Robinson Way, Cambridge, CB2 0RE, UK; Alderley Park, Cheshire, SK10 4TG, UK and AstraZeneca, Unit 310 (Darwin Building), Cambridge Science Park, Milton Road, Cambridge, CB4 0WG, UK.*

[5]*Pelago Bioscience AB, Nobels Väg 3, 17165, Sweden.*

[6]*Current address: Department of Microbiology and Molecular Genetics, University of California, Davis, Briggs Hall, One Shields Ave, Davis, CA 95616-8665, USA.*

Supplementary Results

Supplementary Table 1

Supplementary Table 1. Data collection and refinement statistics

	Crystal 1
Data collection	
Space group	P1
Cell dimensions	
a, *b*, *c* (Å)	43.3, 50.2, 66.9
α, β, γ (°)	102.1, 94.0, 90.7
Resolution (Å)	65.3-2.8 (2.9-2.8)
R_{sym} or R_{merge}	0.09 (0.26)
$I / \sigma I$	6.1 (2.5)
Completeness (%)	92 (91)
Redundancy	1.8 (1.8)
Refinement	
Resolution (Å)	49-2.8
No. reflections	12396
R_{work} / R_{free}	23.3 (27) / 23.7 (37)
No. atoms	4268
Protein	4217
Ligand/ion	50
Water	1
B-factors	
Protein	25
Ligand/ion	45
Water	36
R.m.s. deviations	
Bond lengths (Å)	0.005
Bond angles (°)	1.02

One crystal was used in the experiment.
Highest-resolution shell is shown in parentheses.

Supplementary Results

Supplementary Tables 2–4

Supplementary Table 2. Thermodynamic parameters derived from global fitting of triplicate data using SEDPHAT v10.

Compound	Protein	K_D, nM* (95% C.I.)	n§ (±S.E.)	ΔH† kcal•mol^{-1}	ΔS‡ cal•mol^{-1}•deg^{-1}	χ^{2}¶
1	hFEN1-336	182 (72-395)	1.10 (±0.02)	1.60	36	31
2	hFEN1-336	194 (62-492)	1.05 (±0.01)	1.51	36	30
3	hFEN1-336	1577 (725-3333)	0.75 (±0.03)	1.90	33	35
1	hFEN1-WT	260 (80-687)	1.12 (±0.09)	1.40	35	17
1	hFEN1-R100A	117 (22-387)	1.17 (±0.05)	1.55	37	70

*Dissociation constant (with 95% confidence interval) §Stoichiometry (with standard error) †Molar enthalpy of binding ‡Molar entropy of binding ¶Critical chi-square value for 95% confidence limits from global analysis

Supplementary Table 3. hFEN1-R100A and DF1 equilibrium dissociation constants $K_{D(binding)}$ and $K_{D(bending)}$. Determined by FA and FRET, respectively, under the indicated solution conditions.

Conditions	FA - R100A			FRET - R100A
	r_{min}§	r_{max}¶	$K_{D(Binding)}$, nM	$K_{D(Bending)}$, nM
Ca^{2+}	0.04	0.12	92 ± 10	135 ± 34
Mg^{2+} + **1**	0.02	0.14	311 ± 100	436 ± 74
Mg^{2+} + **2**	0.03	0.13	1033 ± 31	>1000
EDTA	0.03	0.13	111 ± 8	282 ± 76
EDTA + **1**	0.02	0.13	111 ± 6	n.d.

§r_{min} and ¶r_{max} are the anisotropy value of the unbound substrate and at protein saturation, respectively.

Supplementary Table 4. Permeability and logD data for compounds 1–4. Permeability was measured in bidirectional MDCK and Caco-2 assays, and logD via shake-flask method at pH 7.4.

	MDCK P_{app}(AB)/ 1e^{-6} cm/s	**MDCK P_{app}(BA)/ 1e^{-6} cm/s**	**Efflux ratio**	**Caco-2 P_{app}(AB)/ 1e^{-6} cm/s**	**Caco-2 P_{app}(AB)/ 1e^{-6} cm/s**	**Efflux ratio**	**LogD**
1	4.4	12.2	2.8	13.1	5.6	0.4	1.4
2	41.1	7.3	0.18	NT	NT	NT	0.8
3	NT	NT	NT	3.4	4.9	1.4	0.05
4	26.5	2.2	0.084	NT	NT	NT	1.5

Compounds were incubated at 10 µM in cultured MDCK or Caco-2 cells. Permeability was measured in both the apical to basolateral (A to B) and basolateral to apical (B to A) directions. MDCK results are a mean of duplicate measurements; Caco-2 results are from single experiments.

Supplementary Results

Supplementary Tables 5 and 6

Supplementary Table 5. Oligonucleotides used herein.

Oligo	Sequence
5'F1	5'-**FAM**-TTTTTACAAGGACTGCTCGACAC-3'
5'F2	5'-TTTTTACAAGGACTGCTCGACAC-3'
T1	5'-GTGTCGAGCCCTTGTGACGACGAAGTCGTCC-3'
5'F3	5'-TTT TTG (**2AP**)(**2AP**)A GGC AGA GTG-3'
T2	5'-CAC TCT GCC TTT CGA CAG CGA AGC TGT CC-3'
T3	5'-(**TAMRA**)-TGGACGGGTGGCGTTAAGGTTAGGCT-3'
3'F1	5'-(**FAM**)-AGCCTAACCTTAACGG-3'
5'F4	5'-TTTTCCACCCGTCCA-3'
T4	5'-TGGACGGGTGGCGTTAAGGTTAGGCT-3'
3'F2	5'-AGCCTAACCTTAACGG-3'
5'F5	5'-(**FAM**)-TTTTTTTTTTGAGGCAGAGTAGGACC3'
T5	5'-(**BIOTIN**)-GGTCCTACTCTGCCTCAAGAGAGAGACGGTCTGCTGCACTGGATCTGG3'
3'F3	5'-(**BIOTIN**)-CCAGATCCAGTGCAGCAGACCGTCTCTCTCC3'
5'E3	5'-(**FAM**)-ACAAGGACTGCTCGACAC-3'
AB1	5'-GATCTGATTCCCCAACTCCTCTGTTTCACT(**dS**)CTGGACCGCATG-(**FAM**)-3'
AB2	5'-CATGCGGTCCAGTAGTGAAACAGAGGAGTTGGGGAATCAGATC-3'
T6	5'-GTGTCGAGCAGTCCTTGTGACGAC-3'
pY7	5'(**FAM**)GGCTGTCGAACACACACCGCTTGCGGTGTGTGTTCCACAAC-3'
RNA1	5'-/5PHOS/ACU CAC UCA CUC ACC AAA AAA AAA AAA ACC-FAM-3'
DNA1	5′-TAMRA-GGT TTT TTT TTT TTT GG-OH-3′

Sequences of individual oligonucleotides used. (**2AP**): 2-aminopurine, (**FAM**): 5′-fluorescein, (**TAMRA**): 5′-tetramethylrhodamine.

Supplementary Table 6. Oligonucleotide combinations to make various constructs

Construct	Oligonucleotide composition
DF1	$5'F_1 + T_1$
DF2	$5'F_2 + T_1$
NL	$5'F_4 + T_4 + 3'F_2$
DOL	$5'F_4 + T_4 + 3'F_1$
AOL	$5'F_4 + T_3 + 3'F_2$
DAL	$5'F_4 + T_3 + 3'F_1$
DF3	$5'F_3 + T_2$
DF4	$5'F_5 + T_5 + 3'F_3$
SF	$5'E_3 + T_1$
AP1	$AB_1 + AB_2$
EO	$5'E_3 + T_6$
pY7	pY7 (unimolecular hairpin)
RD1	RNA1 + DNA1

The substrates were prepared using the indicated oligonucleotides by heating and annealing of template (T) and flap strand (F or E) oligonucleotides in a ratio of 1.1:1, respectively, in folding buffer (100 mM KCl, 50 mM HEPES pH 7.5). Concentrations of oligonucleotides were determined using extinction coefficients derived from the OligoAnalyzer® Tool (http://eu.idtdna.com/analyzer/Applications). DF-double flap, NL –no label double flap, DOL –donor only label double flap, AOL-acceptor only label double flap, DAL –donor acceptor label double flap, EO-exonuclease substrate with 3'overhang and pY-7-pseudo-Y substrate.

Supplementary Results

Supplementary Figure 1

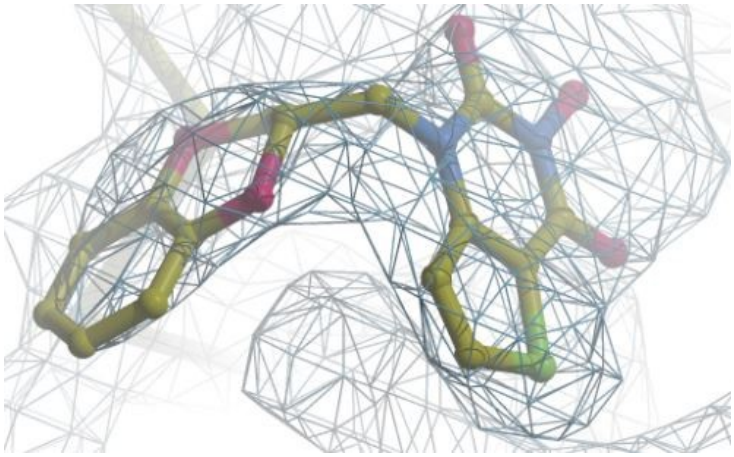

Supplementary Figure 1. Ligand electron density (PDB ID 5FV7).

Supplementary Results

Supplementary Figure 2

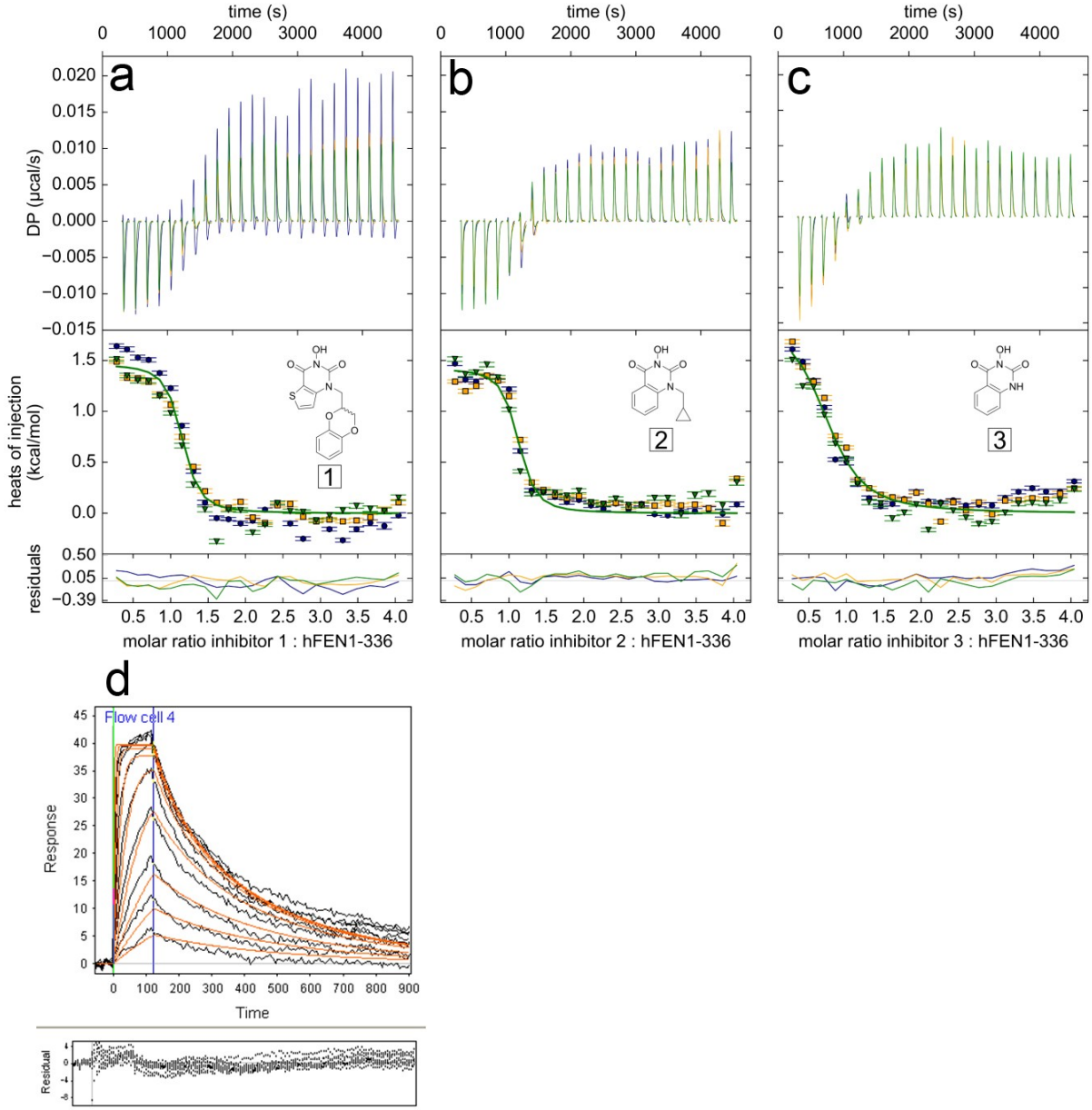

Supplementary Figure 2. Inhibitors binding to hFEN1-336Δ. Affinity of inhibitor (**a**) **1,** (**b**) **2** and (**c**) **3** for hFEN1-336Δ assessed by isothermal titration calorimetry (ITC) at pH 7.5 and 25 °C in the presence of 8 mM Mg^{2+}. The top, middle and bottom panels show the raw data, processed data and residuals, respectively. The orange, blue, and green circles represent data from the three respective replicates used in this analysis. The residual lines in the lower graph are coloured according to their respective replicate. Inserts show the structure of **1**, **2** and **3**[1]. See Supplementary Table 2 for parameters. Data in panels a–c are from three independent experiments with global fitting. (**d**) Association (k_a) and dissociation (k_d) rates of **1** with hFEN1-336Δ-Mg^{2+} measured by SPR. Protein was immobilised using His directional covalent capture onto a Ni-NTA chip to a density of 4800 RU. Compound concentration responses were injected across the protein surface in running buffer composed of 50 mM HEPES pH 7.4, 150 mM NaCl, 50 mM $MgCl_2$, 0.005% P20 (Tween-20). k_{on} = $1.49 \times 10^5 \pm 7.5 \times 10^3$ M^{-1} s^{-1}, k_{off} = 0.00554 ± 0.00041 s^{-1}, yielding K_d = 37.2 ± 4.7 nM, $t_{½(dissociation)}$ = 125 ± 9.3 s (i.e. 2.1 mins) and residence time ($1/k_{off}$) = 180 ± 13 s (i.e. 3 mins).

Supplementary Results

Supplementary Figure 3

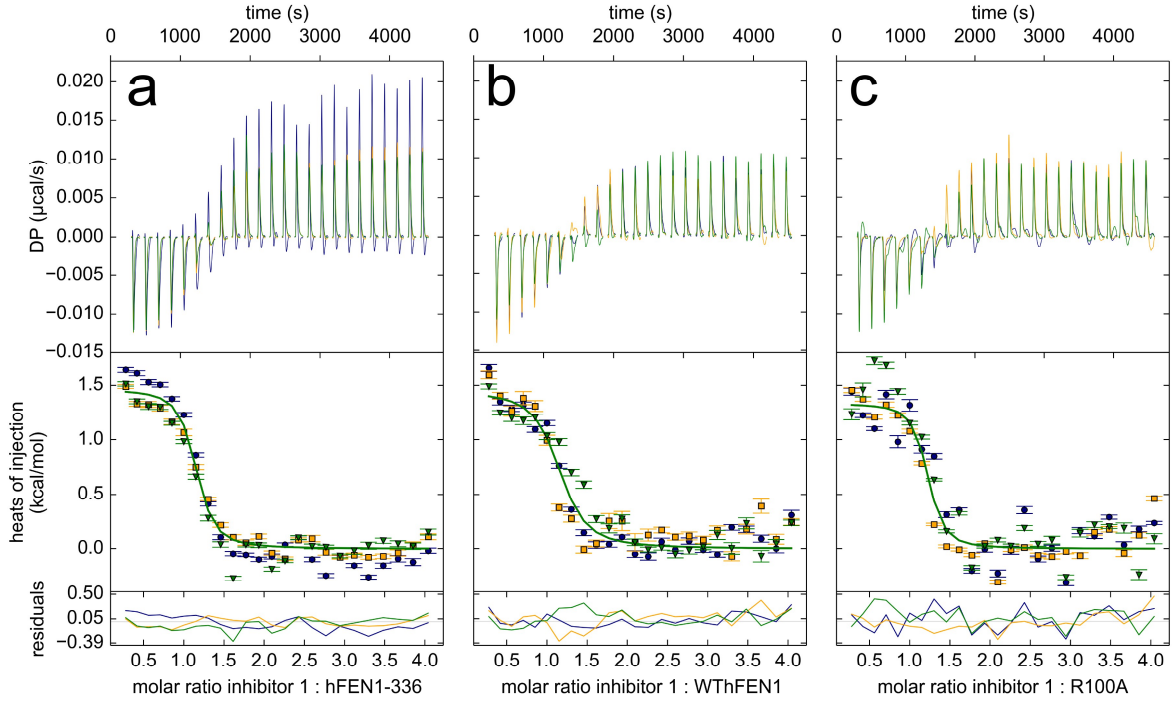

Supplementary Figure 3. Comparison of inhibitor 1 binding to hFEN1-336Δ, full length (WT) hFEN1 and hFEN1R100A. (**a**) Affinity of inhibitor **1** for hFEN1-336Δ assessed by isothermal titration calorimetry (ITC). n = 1.10 ± 0.02, K_D = 182 nM (95% CL, 72-395 nM), ΔH = 1.60 kcal/mol, ΔS = 36 cal/mol/deg, χ^2 = 31. (**b**) Affinity of inhibitor **1** for WThFEN1 assessed by isothermal titration calorimetry (ITC). n = 1.05 ± 0.03, K_D = 194 nM (95% CL, 62-492 nM), ΔH = 1.51 kcal/mol, ΔS = 55 cal/mol/deg, χ^2 = 30. (**c**) Affinity of inhibitor **1** for hFEN1R100A assessed by isothermal titration calorimetry (ITC). n = 1.17 ± 0.05, K_D = 117 nM (95% CL, 22-387 nM), ΔH = 1.55 kcal/mol, ΔS = 37 cal/mol/deg, χ^2 = 70. The top, middle and bottom panels show the raw data, processed data and residuals, respectively. The orange, blue, and green circles represent data from the three respective replicates used in this analysis. The residual lines in the lower graph are colored according to their respective replicate. Each measurement was conducted at pH 7.5 and 25 ˚C in the presence of 8 mM Mg^{2+}. Parameters quoted are from global analysis of the triplicate experiments. n-stoichiometry, K_D-dissociation constant (95% confidence limits), ΔH-enthalpic change, ΔS-entropic change and χ^2 critical chi-square value for 95% limits on global analysis.

Supplementary Results

Supplementary Figure 4

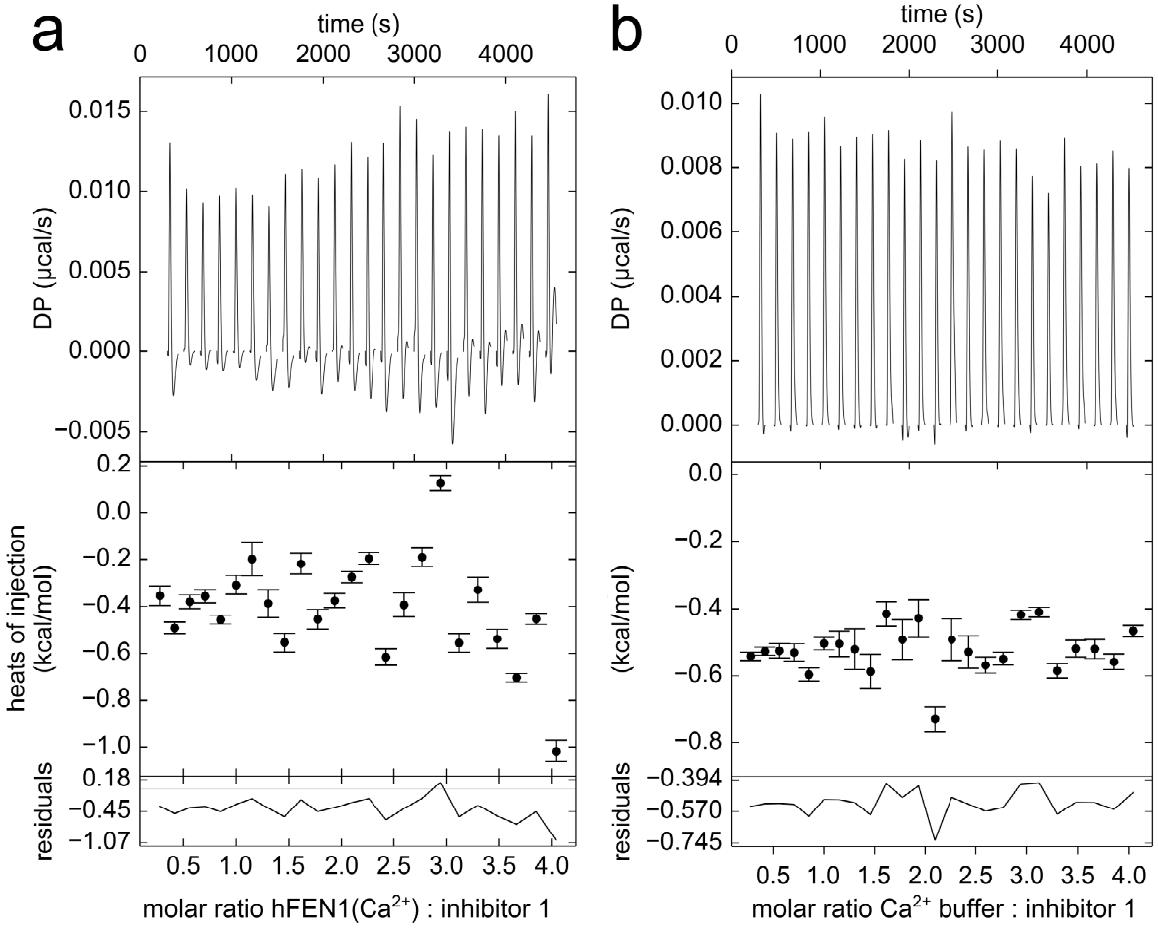

Supplementary Figure 4. Inhibitor 1 binding to hFEN1-336Δ in the presence of Ca^{2+} ions. (**a**) Titration of inhibitor **1** into hFEN1-336Δ in the presence of 10 mM Ca^{2+}. (**b**) Titration of inhibitor **1** into Ca^{2+} containing buffer. The top, middle and bottom panels show the raw data, processed data and residuals, respectively. Individual titrations, each conducted at pH 7.5 and 25 °C. The data presented is from a single experiment in each panel (**a** and **b**), with error bars representing the error associated with integration. A second experiment for each set of conditions was carried out with similar results (data from these repeats is not shown).

Supplementary Results

Supplementary Figure 5

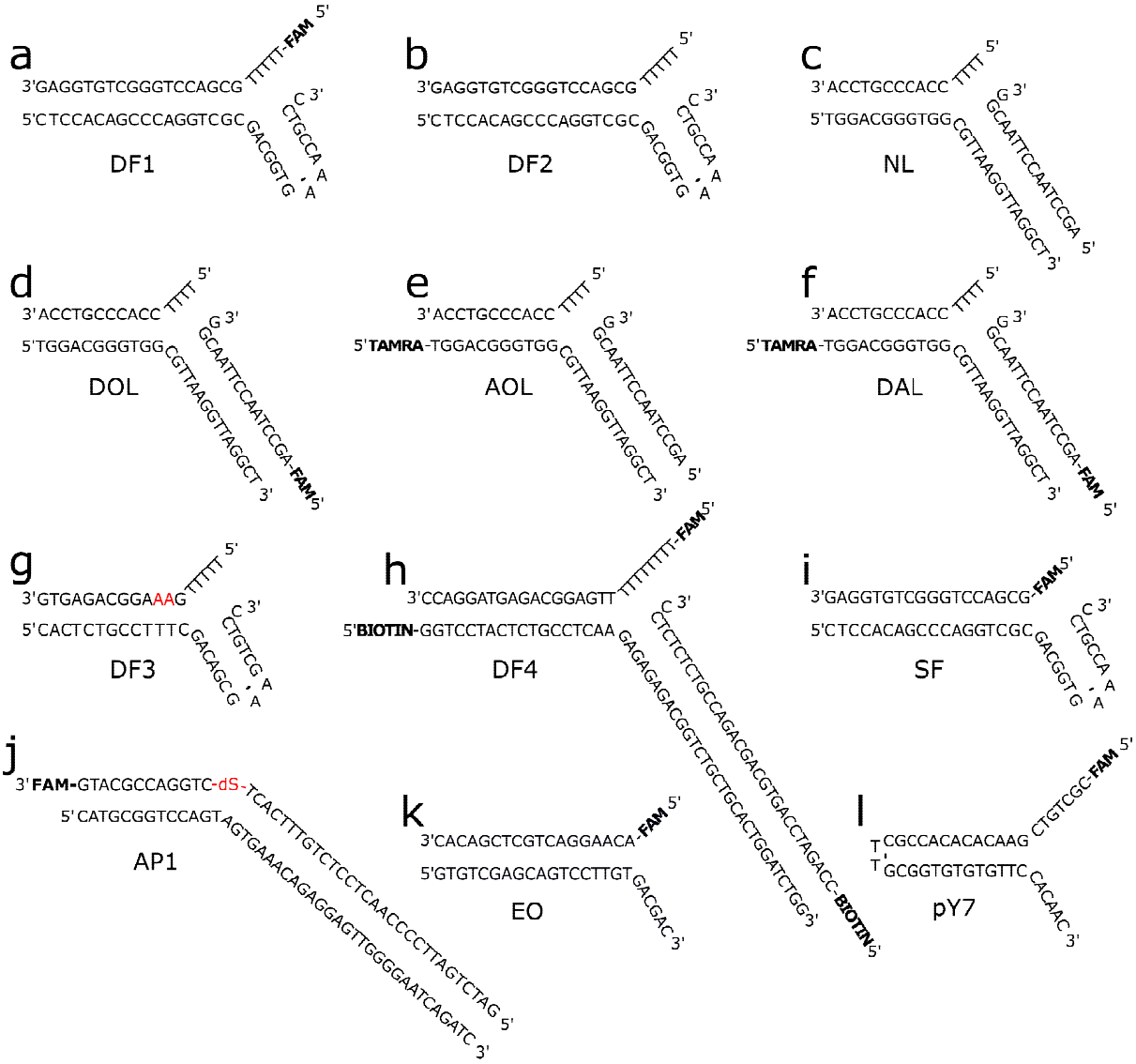

Supplementary Figure 5. Schematic representation of oligonucleotide constructs listed in Table S6. (**a**) Double flap 1 (DF1) with associated 5'-FAM label for kinetics and fluorescence anisotropy (FA) studies. (**b**) Unlabelled double flap (DF2) for competition experiments in FA. (**c**–**f**) Constructs used in FRET studies: (**c**) NL –no label, (**d**) DOL –donor only label, (**e**) AOL, acceptor only label and (**f**) DAL –donor acceptor label. (**g**) Double flap (DF3) for low energy CD studies. Location of tandem 2-aminopurines is indicated in red. (**h**) Double flap (DF4) for kinetic experiments involving hPCNA, with 5'-FAM label. (**i**) Single flap (SF) with 5'-FAM label used for kinetic studies. (**j**) APE1 substrate with 3'-FAM label and a dSpacer CE phosphoramidite labelled dS. (**k**) Exonuclease substrate (EO) labelled with 5'-FAM for kinetic studies with hEXO1-352. (**l**) PseudoY substrate (pY7) used for kinetic studies with T5 FEN.

Supplementary Results

Supplementary Figure 6

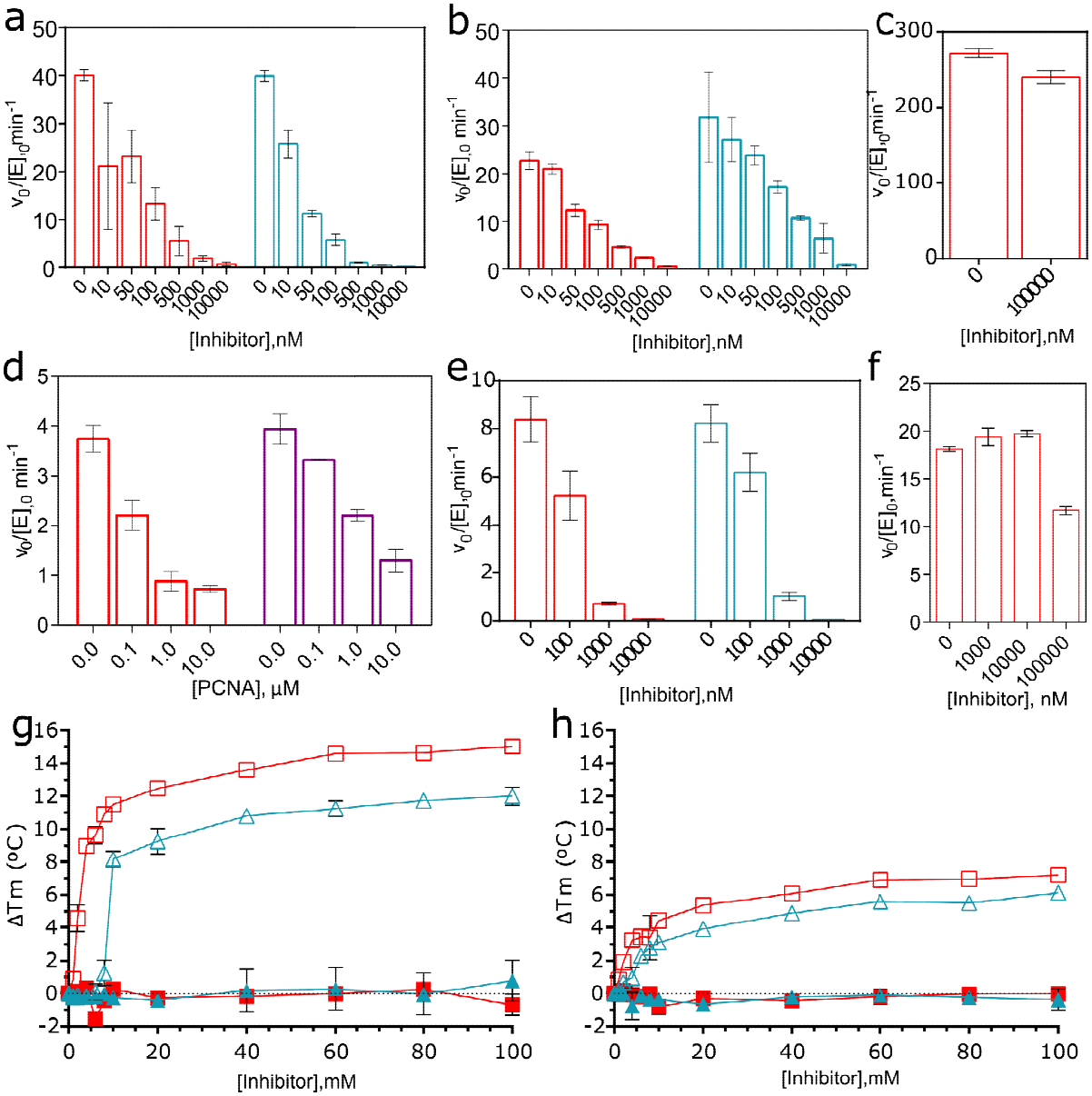

Supplementary Figure 6. Inhibition and binding of compounds to hFEN1 and other 5′-nucleases. (**a**–**f**) The rate of reaction catalysed by (**a-b**) hFEN1, (**c**) T5FEN, (**d**) hFEN1 with PCNA, (**e**) hEXO1 and (**f**) hAPE1 in the presence of varying concentrations of compound **1** (red), compound **2** (blue) and compound **4** (purple). Measurements are the average (n=3) multiple turnover rates of reaction with optimal substrates and buffers for the respective proteins (*i.e*, (**a**) double flap (DF1), (**b**) single flap (SF), (**c**) pseudo-Y (pY7) structure[2], (**d**) double flap (DF4), (**e**) 3′-overhang (EO) and (**f**) abasic site substrate (AP1); Supplementary Figure 5a,h,i. Error bars represent the SEM. The concentrations of substrate were 150 nM in (**a**–**b, e**–**f**), 35 nM in (**c**) and 50 nM in (**d**). Notably, the reactions of hFEN1 and hEXO1 are inhibited by the *N*-hydroxyureas, whereas the reaction catalysed by the related 5′-nuclease T5FEN is not. (**g**–**h**) Binding of **1** (red) and **2** (blue) to (**g**) hFEN1 and (**h**) hEXO1 measured by differential scanning fluorimetry (DSF) using Sypro® Orange. Experiments contained 2.5 µM protein, 1× Sypro Orange, 50 mM HEPES pH 7.5, 100 mM KCl, 8 mM $MgCl_2$ and either 25 mM EDTA (closed symbols) or 25 mM NaCl (open symbols). Measurements represent average difference (n=3) in melting temperature (ΔT_m) compared to control with error bars representing SEM. Notably, stabilization of the protein by either **1** or **2** is dependent on the presence of free Mg^{2+} (*i.e*. no EDTA).

Supplementary Results

Supplementary Figure 7

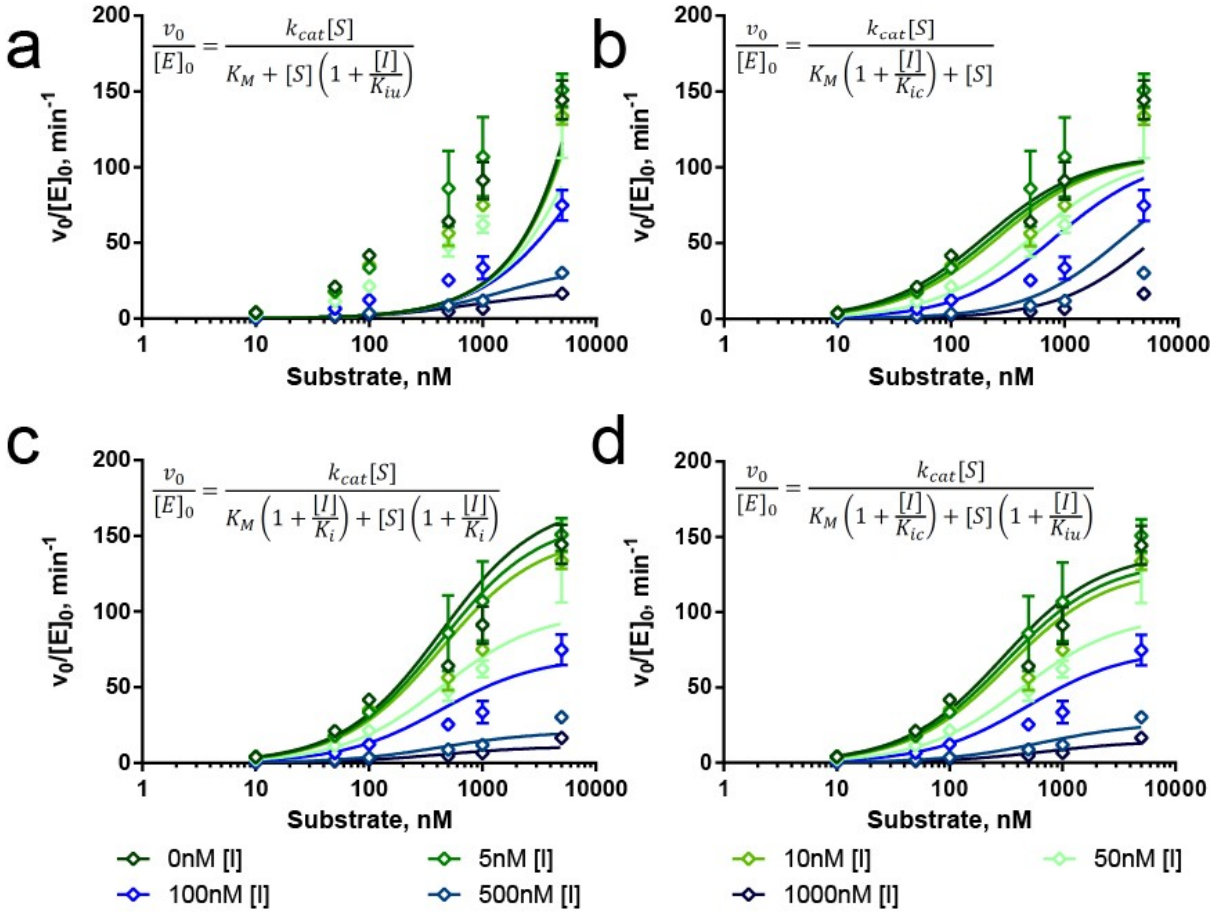

e

Inhibition Model	k_{cat}, min^{-1} (±S.E.)	K_M, nM (±S.E.)	K_{ic}, nM (±S.E.)	K_{iu}, nM (±S.E.)	ΔAIC_c vs Mixed (P-value)
Uncompetitive	amb.	amb.	n.a.	amb.	n.a.
Competitive	108 ± 7	200 ± 26	31 ± 4	n.a.	75.91 (<0.0001)
Non-Competitive	173 ± 10	433 ± 33	68 ± 5	68 ± 5	24.76 (<0.0001)
Mixed	140 ± 9	297 ± 31	48 ± 5	117 ± 27	n.a.

Supplementary Figure 7. Comparison of non-linear regression fitting of inhibitor 1 kinetic data to kinetic inhibition models. (**a**–**d**) Plots of normalized initial rate ($v_0/[E]_0$ (min^{-1}) vs. substrate concentration for hFEN1-336Δ-catalyzed hydrolysis of DF1 (Supplementary Figure 5a) in the presence of a range of inhibitor **1** concentrations (see legend for colour coding) showing the non-linear regression results associated with the indicated inhibition model: (**a**) Uncompetitive, (**b**) Competitive, (**c**) Non-competitive, and (**d**) Mixed. The open diamonds represent the mean of at least three repeats, and the error bars represent the standard error of the mean. The equation for each model is shown as an inset in the respective plot. (**e**) Table showing the kinetic parameters from non-linear regression analysis for each inhibition model. The uncompetitive model was not able to converge, and thus, the parameters are ambiguous (amb.). k_{cat}-turnover rate, K_M-complex term associated with affinity for all enzyme bound species, K_{ic}-affinity of I for free E, and K_{iu}-affinity of I for ES. Errors represent standard error of the mean (S.E.). ΔAIC_C is the difference between second order (corrected) Aikake Information Criteria values for each successful fit versus the more complicated mixed inhibition value. The low P-value for mixed inhibition strongly suggests this as the best explanatory model (see online methods for more detail).

Supplementary Results

Supplementary Figure 8

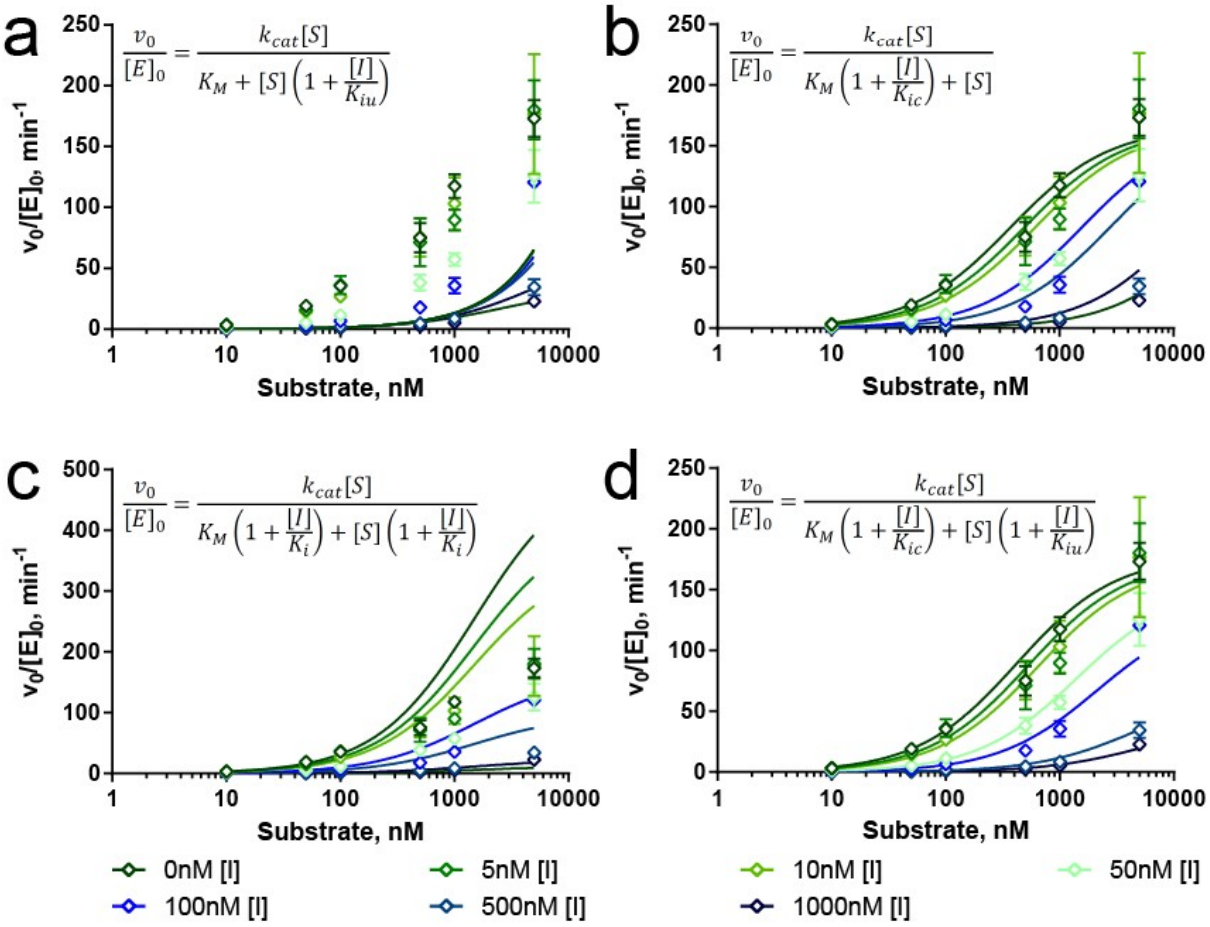

e

Inhibition Model	k_{cat}, min^{-1} (±S.E.)	K_M, nM (±S.E.)	K_{ic}, nM (±S.E.)	K_{iu}, nM (±S.E.)	ΔAIC_c vs Mixed (P-value)
Uncompetitive	amb.	amb.	n.a.	amb.	n.a.
Competitive	169 ± 11	374 ± 43	16 ± 2	n.a.	10.21 (<0.0005)
Non-Competitive	amb.	amb.	amb.	amb.	n.a.
Mixed	182 ± 13	422 ± 50	17 ± 2	306 ± 125	n.a.

Supplementary Figure 8. Comparison of non-linear regression fitting of inhibitor 2 kinetic data to inhibition models. (**a-d**) Plots of normalized initial rate ($v_0/[E]_0$ (min^{-1}) vs. substrate concentration for hFEN1-336Δ hydrolysis of DF1 (Supplementary Figure 5a) in the presence of a range of inhibitor **2** concentrations (see legend for colour coding) showing the non-linear regression results associated with the indicated inhibition model: (**a**) Uncompetitive, (**b**) Competitive, (**c**) Non-competitive, and (**d**) Mixed. The open diamonds represent the mean of at least three repeats, and the error bars represent the standard error of the mean. The equation for each model is shown as an inset in the respective plot. (**e**) Table showing the kinetic parameters from non-linear regression analysis for each inhibition model. The uncompetitive non-competitive models were not able to converge, and thus, the parameters are ambiguous (amb.). Some parameters are not applicable (n.a.) to the model. k_{cat}-turnover rate, K_M-complex term associated with affinity for all enzyme bound species, K_{ic}-affinity of I for free E, and K_{iu}-affinity of I for ES. Errors represent standard error of the mean (S.E.). ΔAIC is the difference between Aikake Information Criteria values for each successful fit versus the more complicated mixed inhibition value. Mixed inhibition is the better model statistically as indicated by the low P-value (see online methods for more detail).

Supplementary Results

Supplementary Figure 9

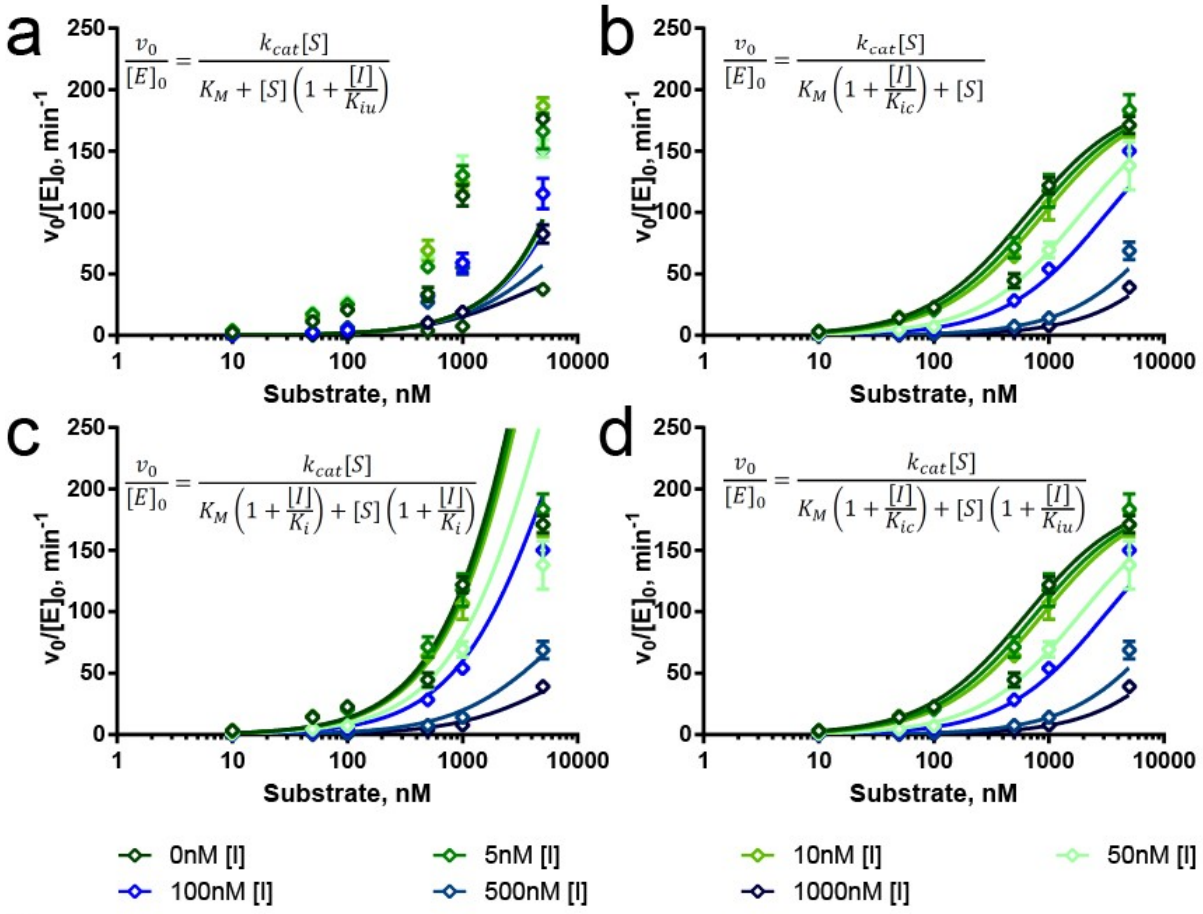

e

Inhibition Model	k_{cat}, min^{-1} (±S.E.)	K_M, nM (±S.E.)	K_{ic}, nM (±S.E.)	K_{iu}, nM (±S.E.)	ΔAIC$_c$ vs Mixed (P-value)
Uncompetitive	amb.	amb.	n.a.	amb.	n.a.
Competitive	194.5 ± 11	631 ± 53	26.0 ± 1.7	n.a.	n.a.
Non-Competitive	amb.	amb.	amb.	amb.	n.a.
Mixed	194.5 ± 11	631 ± 53	26.0 ± 1.7	amb.	n.a.

Supplementary Figure 9. Comparison of non-linear regression fitting of inhibitor 4 kinetic data to inhibition models. (**a**–**d**) Plots of normalized initial rate ($v_0/[E]_0$ (min^{-1}) vs. substrate concentration for hFEN1-336Δ hydrolysis of DF1 (Supplementary Figure 5a) in the presence of a range of inhibitor **4** concentrations (see legend for colour coding) showing the non-linear regression results associated with the indicated inhibition model: (**a**) Uncompetitive, (**b**) Competitive, (**c**) Non-competitive, and (**d**) Mixed. The open diamonds represent the mean of global fitting from two independent triplicate experiments (i.e. N = 2, n = 6), and the error bars represent the standard error of the mean. The equation for each model is shown as an inset in the respective plot. (**e**) Table showing the kinetic parameters from non-linear regression analysis for each inhibition model. The uncompetitive non-competitive models were not able to converge, and thus, the parameters are ambiguous (amb.). Some parameters are not applicable (n.a.) to the model. k_{cat}-turnover rate, K_M-complex term associated with affinity for all enzyme bound species, K_{ic}-affinity of I for free E, and K_{iu}-affinity of I for ES. Errors represent standard error of the mean (S.E.). ΔAIC is the difference between Aikake Information Criteria values for each successful fit versus the more complicated mixed inhibition value. Competitive inhibition is the better model as it is the only one that can be fit to the data (see online methods for more detail).

Supplementary Results

Supplementary Figure 10

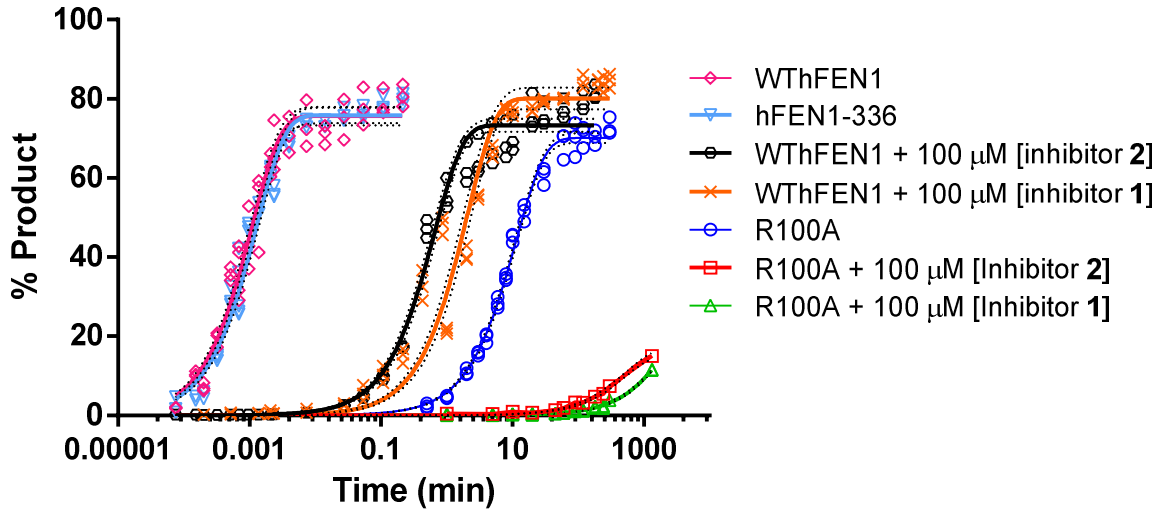

Supplementary Figure 10. Hydrolysis of substrate DF1 by FEN1 proteins under single turnover conditions, in the presence and absence of inhibitors. (**a**) Maximal single turnover rate profiles (% conversion *vs.* time) for cleavage of DF1 (Supplementary Figure 5a) measured at 37 °C, pH 7.5 in the presence of Mg^{2+} (note log scale of x-axis) fitted to equation 1 (online methods). Magenta plot (open diamonds), full length hFEN1 no inhibitor, k_{ST} = 916 ± 49 min^{-1}; cyan plot (inverted open triangles), hFEN1-336Δ no inhibitor, k_{ST} = 755 ± 35 min^{-1}; orange plot (crosses), hFEN1 plus 100 μM inhibitor **1,** k_{ST} = 0.48 ± 0.04 min^{-1}; black plot (open circles) hFEN1 plus 100 μM inhibitor **2,** k_{ST} = 1.52 ± 0.09 min^{-1}; blue plot (open circles) hFEN1-R100A, no inhibitor k_{ST} = 0.087 ± 0.003 min^{-1}; green plot (open triangles), hFEN1-R100A plus 100 μM inhibitor **1,** k_{ST} = ~4 × 10^{-4} min^{-1}; red plot (open squares), hFEN1-R100A plus 100 μM inhibitor **2,** k_{ST} = ~2 × 10^{-3} min^{-1}. In each case, dashed black lines represent 95% confidence interval of the fit. All plots represent triplicate measurements (technical replicates).

Supplementary Results

Supplementary Figure 11

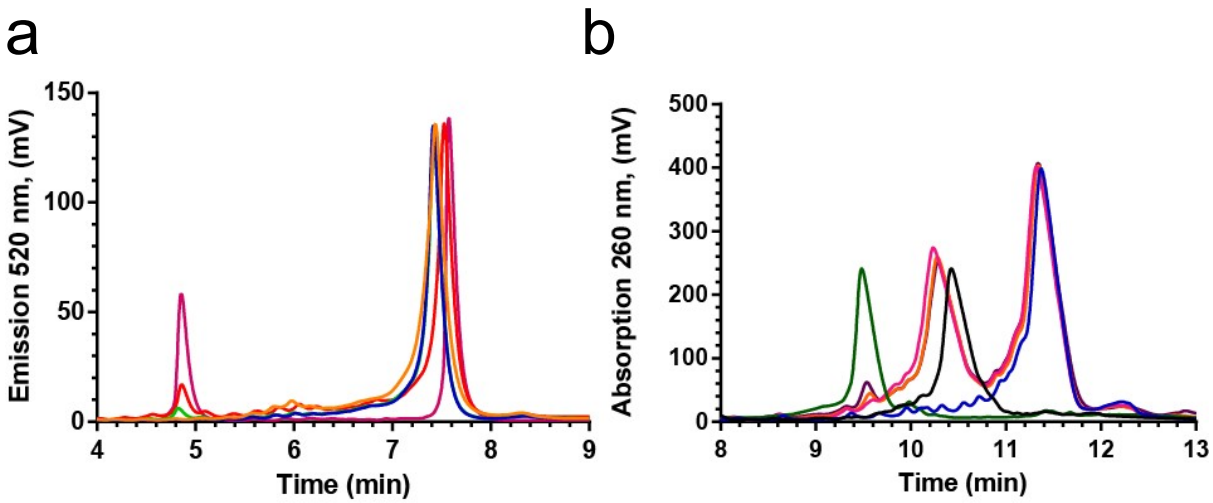

Supplementary Figure 11. Denaturing HPLC (dHPLC) traces to show the amount of product produced after the fluorescence anisotropy and ECCD experiments to determine the K_D of DF1 and unpairing ability, respectively, for hFEN1-R100A in the presence of 8 mM $MgCl_2$ and 100 µM inhibitor 1 and 2. (**a**) The orange trace is unreacted DF1, and the magenta trace is DF1 reacted with hFEN1-WT in the presence of Mg^{2+} to show where the product is expected to elute. The blue, green and red traces are samples taken after fluorescence anisotropy experiments of DF1 with R100A in the presence of 10 mM Ca^{2+}, 8 mM Mg^{2+} and inhibitor **1**, and 8 mM Mg^{2+} and inhibitor **2**, respectively. After fluorescence analyses, an aliquot of each sample was diluted in 8 M urea and 80 mM EDTA to a final concentration of 100 nM for examination by dHPLC. Retention times for the product and the uncleaved flap are approximately 4.9 min and 7.6 min, respectively. (**b**) The blue trace is oligo T2 (Supplementary Table 5), the black trace is unreacted flap strand 5'F_3 and the green trace is the product of 5'F_3 (Supplementary Table 5) reacted with hFEN1-WT in the presence of Mg^{2+} to show where the product is expected to elute. The magenta, orange and purple traces are samples taken after ECCD of R100A in the presence of 10 mM Ca^{2+}, 8 mM Mg^{2+} and inhibitor **1**, and 8 mM Mg^{2+} and inhibitor **2**, respectively. After ECCD analyses, an aliquot of each sample was diluted in 8 M urea and 80 mM EDTA to a final concentration of 5 µM. Retention times for the product and the uncleaved flap are approximately 9.5 min and 10.4 min, respectively. Denaturing HPLC was performed on a WAVE® system, Transgenomic, UK equipped with UV detector using tetrabutylammonium bromide containing buffers and a linear gradient of acetonitrile as described.[3]

Supplementary Results

Supplementary Figure 12

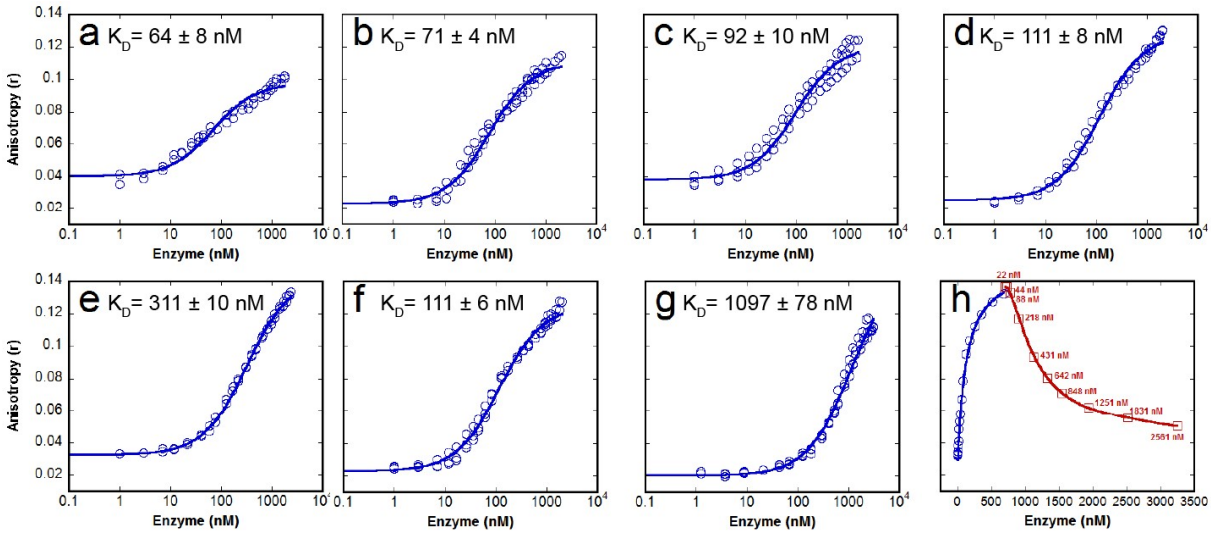

Supplementary Figure 12. DF1 fluorescence anisotropy binding curves and competition experiment. Plots of anisotropy (*r*) of DF1 (Supplementary Figure 5a) as a function of (**a**)–(**b**) WThFEN1 and (**c**)–(**g**) hFEN1-R100A concentrations in (**a**) 10 mM Ca^{2+}, (**b**) 2 mM EDTA, (**c**) 10 mM Ca^{2+}, (**d**) 2 mM EDTA, (**e**) 8mM Mg^{2+} and 100 μM Inhibitor 1, (**f**) 2 mM EDTA and 100 μM Inhibitor 1 and (**g**) 8mM Mg^{2+} and 100 μM Inhibitor 2. Apart from the specified conditions, assays were performed in 110 mM KCl, 55 mM HEPES pH=7.5, 1 mM DTT and at 37 °C. The triplicate data set (open blue circles) is globally fit to equation 7. The K_D value for each condition is shown in the insert of the particular graph. (**h**) In presence of 100 μM inhibitor **1,** hFEN1-R100A was titrated into substrate DF1 (also in presence of 100 μM inhibitor **1**) until ~80% saturation (open-circles, blue) was achieved. Unlabelled competitor DF2 (Figure S5b) in presence of 100 μM inhibitor **1** was then titrated to complete with the labelled DNA (open red squares). The final concentrations associated with competitor DNA at each point are shown next to their respective data points.

Supplementary Results

Supplementary Figure 13

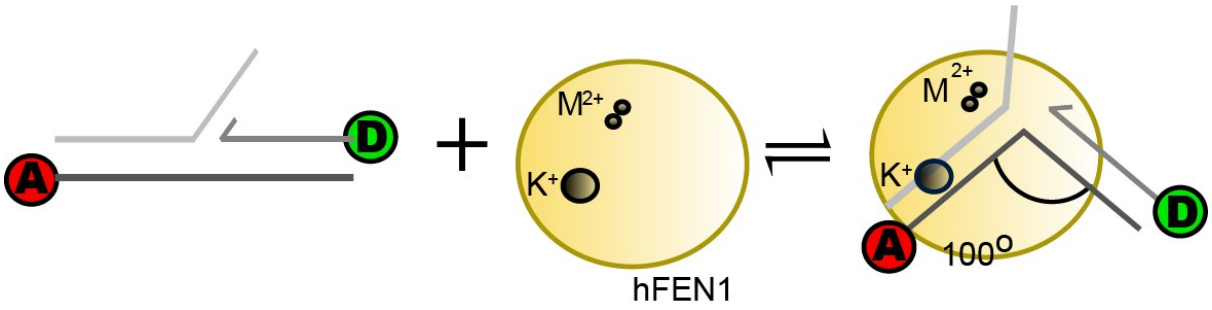

Supplementary Figure 13. Effect of inhibitors on substrate binding assessed by fluorescence anisotropy (FA) and FRET. Schematic representation of FRET dye-pair labelled substrate and conformational changes on binding to hFEN1 measured in Figure 3b. Substrates are constructed and shown schematically according to Supplementary Tables 2,3 and Supplementary Figure 5a,c–f.

Supplementary Results

Supplementary Figure 14

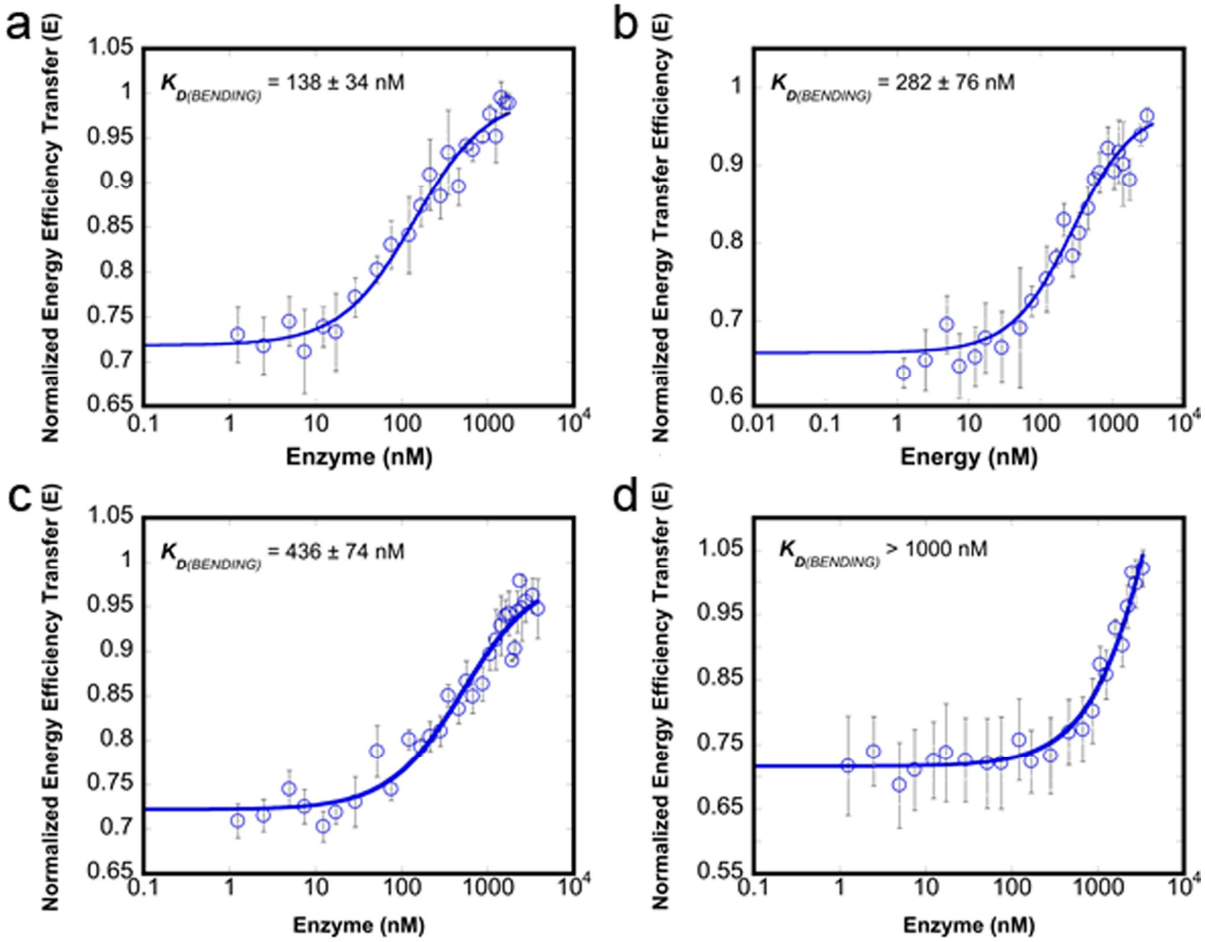

Supplementary Figure 14. Bending dissociation constants DF substrate determined by ensemble FRET measurement for hFEN1-R100A in (a) 10 mM Ca^{2+}, (b) 2 mM EDTA, (c) 8mM Mg^{2+} and 100 µM Inhibitor 1, and (d) 8mM Mg^{2+} and 100 µM Inhibitor 2. Apart from the specified conditions, assays were performed in 110 mM KCl, 55 mM HEPES pH=7.5, 1 mM DTT and at 37 °C. The data points are fit to equation 9 (online methods).The $K_{D(BENDING)}$ value for each condition is shown in the insert of the particular graph, each $K_{D(BENDING)}$ is representative of three independent titrations, and errors shown are standard error.

Supplementary Results

Supplementary Figure 15

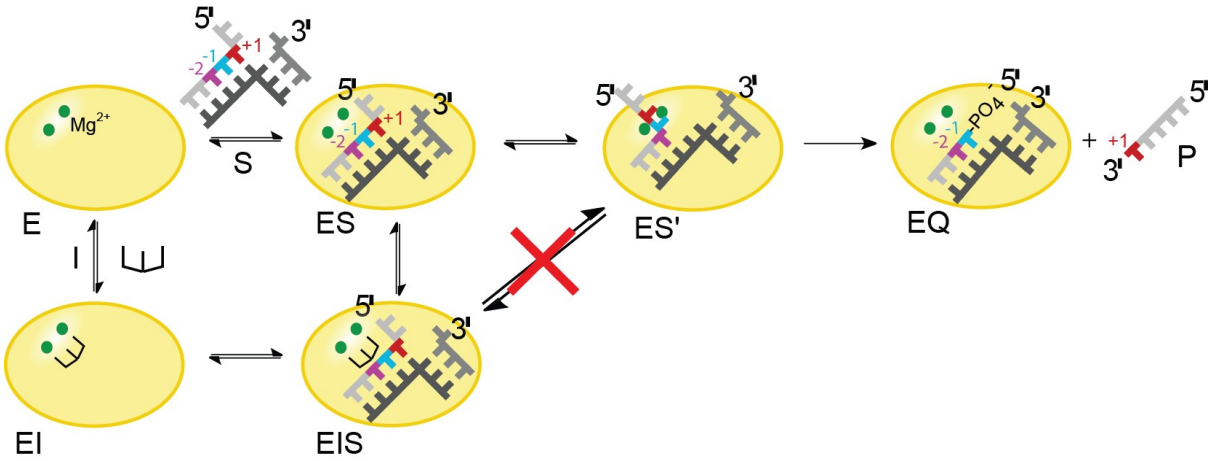

Supplementary Figure 15. *N*-Hydroxyurea inhibitor 1 prevents FEN1 reaction by blocking substrate unpairing. Schematic representation of mixed inhibition by compounds **1** and **2**. When inhibitor is not bound, association of hFEN1 and the double-flap substrate produces an enzyme–DNA complex (ES), whereupon the DNA and enzyme undergo a conformational change (ES') to place the scissile phosphate on the catalytic active-site metal ions (DNU). Phosphate diester hydrolysis is then enabled to cleave the 5'-flap resulting in nicked DNA–enzyme complex (EQ) and single-stranded DNA (P) products. When the *N*-hydroxyurea inhibitor (I) is bound to the Mg^{2+} ions in the hFEN1 active site (EI), the substrate DNA is still able to bind, producing a non-productive enzyme–inhibitor–substrate complex (EIS). The inhibitor in the active site sterically blocks unpairing, thereby preventing hFEN1 catalysis.

Supplementary Results

Supplementary Figure 16

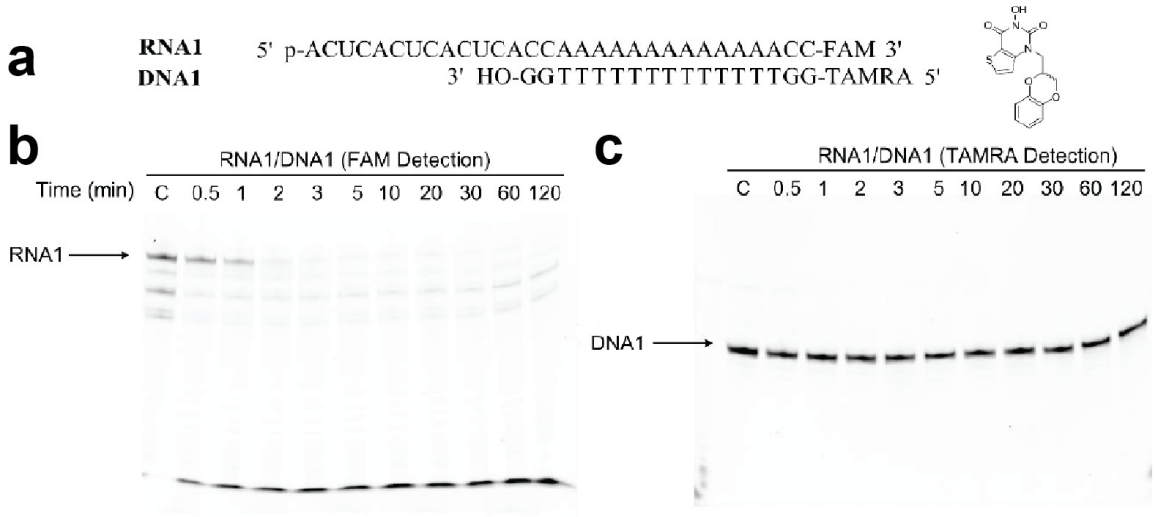

Supplementary Figure 16. XRN1 activity on a RNA:DNA duplex with a 5′-overhang is not inhibited by *N*-hydroxyurea compound 1. (**a**) A schematic of the 5′-overhang RNA/DNA hybrid substrate used[4] and compound **1** is shown. The RNA strand has a 5′-monophosphate and a 3'-FAM for detection, whereas the DNA strand has 5'-TAMRA that prevents reaction on the DNA strand and is used for detection. Reactions were performed at 37 °C with 500 nM substrate, 50 nM enzyme and 100 μM inhibitor **1** (see online methods for conditions). (**b**) Pre-incubation of XRN1 and inhibitor **1** was carried out on ice. A time-course of the reaction is shown with the numbers above each lane representing minutes after initiation with XRN1. Before reaction was initiated, an aliquot of the reaction mixture was removed as a control and is shown in the lane denoted C. Reactions were analysed on a 20% denaturing gel, and (**b**) RNA1 and (**c**) DNA1 products imaged by detecting FAM and TAMRA, respectively. The image here is representative of the result of three independent measurements.

Supplementary Results

Supplementary Figure 17

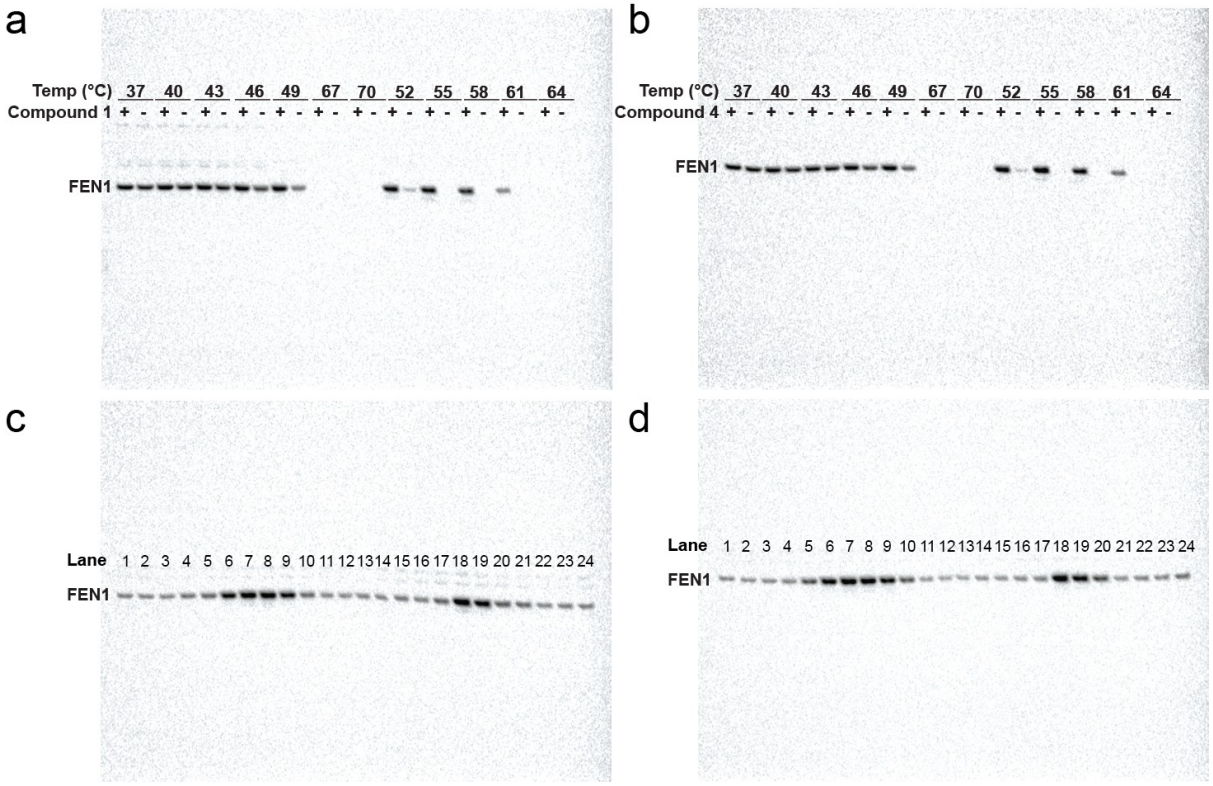

Supplementary Figure 17. Typical blot results used to generate melt and dose response curves shown in Figure 5b,c. Examples of full blots obtained for melt curves with compounds (**a**) **1** and (**b**) **4** at 100 μM. Examples of full blot images of dose response curves obtained at 50 °C with compounds (**c**) **1** and (**d**) **4** at various concentrations. Concentrations of compound used are indicated by the lane number. Lane 1 – 100 pM, 2 – 1 nM, 3 – 10 nM, 4 – 100 nM, 5 – 1 μM, 6 – 10 μM, 7 – 100 μM, 8 – 100 μM, 9 – 10 μM, 10 – 1 μM, 11 – CTRL, 12 – CTRL, 13 – CTRL, 14 – 100 pM, 15 – 1 nM, 16 – 10 nM, 17 – 100 nM, 18 – 100 μM, 19 – 10 μM, 20 – 1 μM, 21 – 100 nM, 22 – 10 nM, 23 – 1 nM, 24 – 100 pM.

Supplementary Results

Supplementary Figure 18

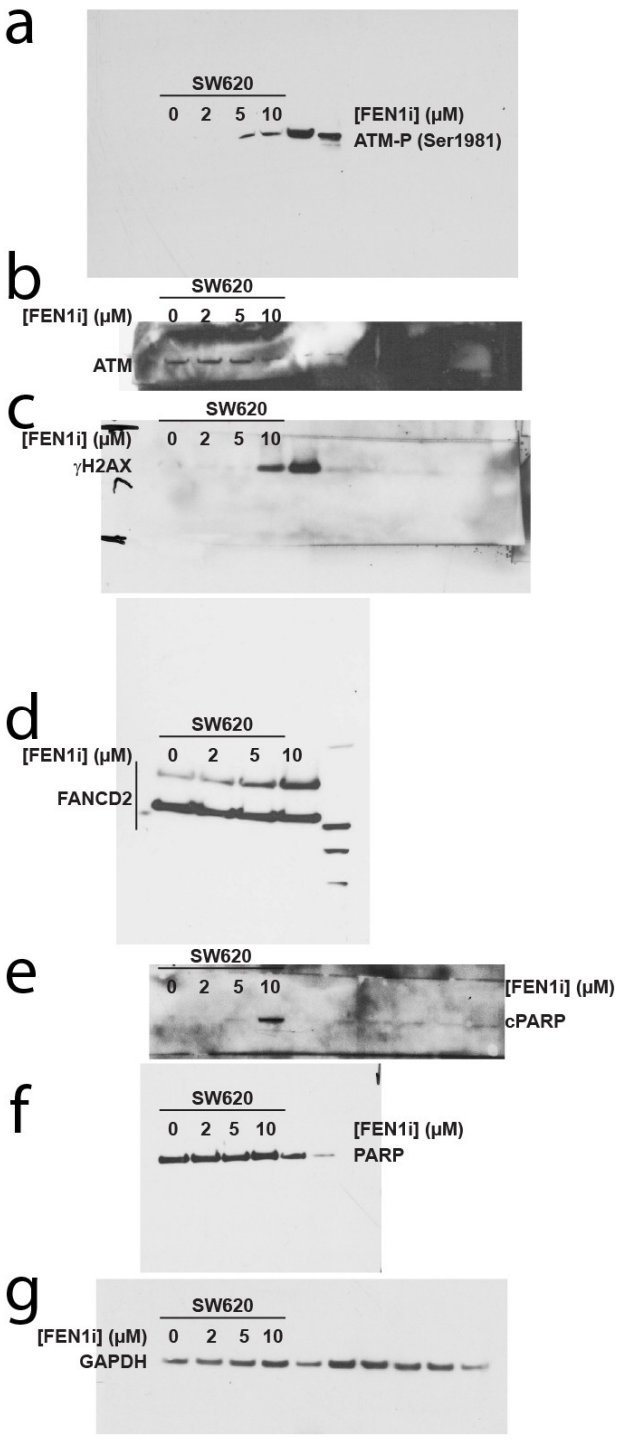

Supplementary Figure 18. Original blots used to generate Figure 5h. (**a**–**g**) Images were taken using Cell Biosciences FlourchemQ imaging platform. Unlabelled bands are from unrelated experiments run in parallel. Antibodies used in these experiments are listed in the online methods**.**

Supplementary Results

Supplementary Figure 19

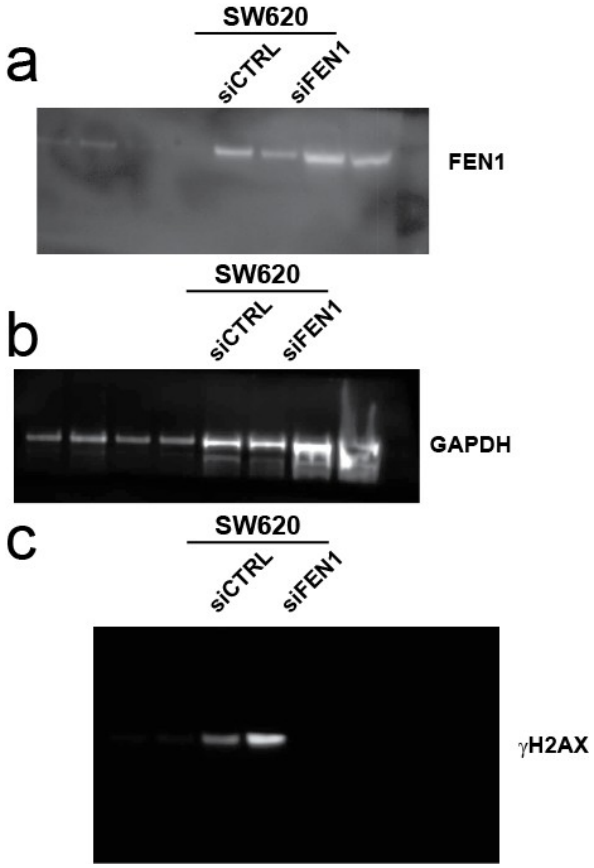

Supplementary Figure 19. Original blots used to generate Figure 5h blot panels. (**a-c**) Images were taken using Cell Biosciences FlourchemQ imaging platform. Unlabelled bands are from unrelated experiments run in parallel. Antibodies used in these experiments are listed in the online methods.

Supplementary Results

Supplementary Figure 20

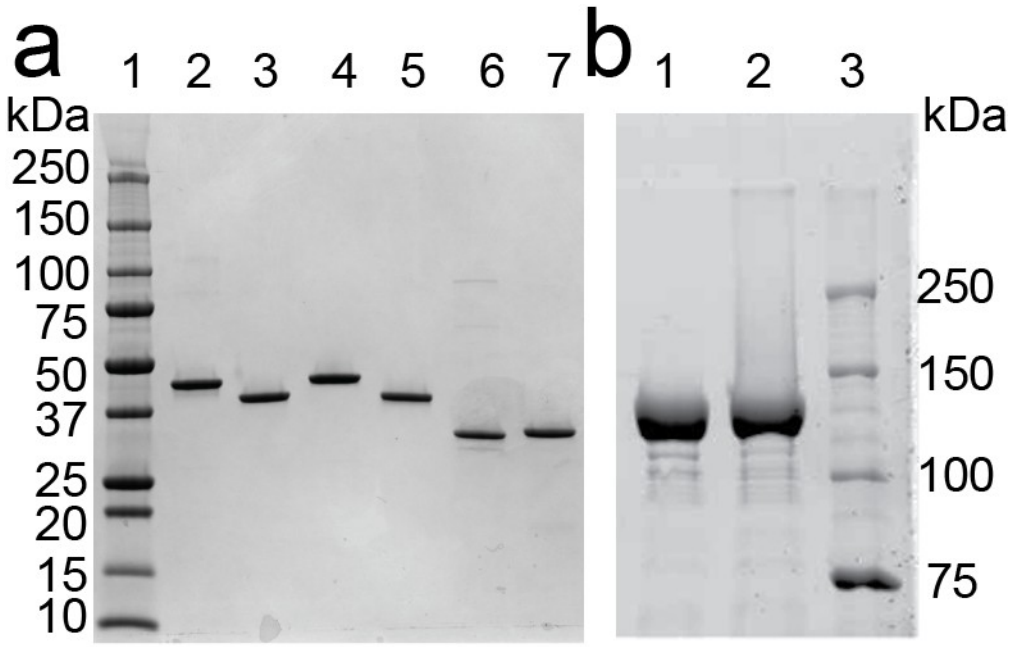

Supplementary Figure 20. SDS-PAGE analysis of the proteins used herein. (**a**) Mini-Protean TGX 4-20% gradient Tris-HCl (Bio-Rad) gel stained with coomassie blue showing the purity of the proteins used in this study. Lane 1 contains the molecular weight marker (Precision Plus AllBlue, Biorad) with the molecular weight shown next to it. Approximately 1 ug of the indicated protein was loaded in each lane: Lane 2 – hFEN1 WT (43.4 kDa), Lane 3 - hFEN1-336 (38.6 kDa), Lane 4 – hFEN1 R100A (43.3 kDa), Lane 5 – hEXO1-352 (40.4 kDa), Lane 6 – T5FEN (33.5 kDa), Lane 7 – hPCNA (30.0 kDa). (**b**) Mini-Protean 7.5% (37.5-1) discontinuous Tris-Glycine gel to show the purity of the *K. lactis* Xrn1 (125 kDa). Lane 1 - 2 ug of protein, Lane 2 – 4 ug of protein, Lane 3 – Molecular weight marker.

Supplementary Results

References for Supplementary Results

1 Tumey, L. N. *et al.* The identification and optimization of a *N*-hydroxy urea series of flap endonuclease 1 inhibitors. *Bioorg. Med. Chem. Lett.* **15**, 277-281, doi:10.1016/j.bmcl.2004.10.086 (2005).

2 Patel, N. *et al.* Flap endonucleases pass 5'-flaps through a flexible arch using a disorder-thread-order mechanism to confer specificity for free 5'-ends. *Nucleic Acids Res.* **40**, 4507-4519, doi:10.1093/nar/gks051 (2012).

3 Finger, L. D. *et al.* The 3′-Flap Pocket of Human Flap Endonuclease 1 Is Critical for Substrate Binding and Catalysis. *J. Biol. Chem.* **284**, 22184-22194, doi:10.1074/jbc.M109.015065 (2009).

4 Sinturel, F. *et al.* Real-time fluorescence detection of exoribonucleases. *RNA* **15**, 2057-2062, doi:10.1261/rna.1670909 (2009).